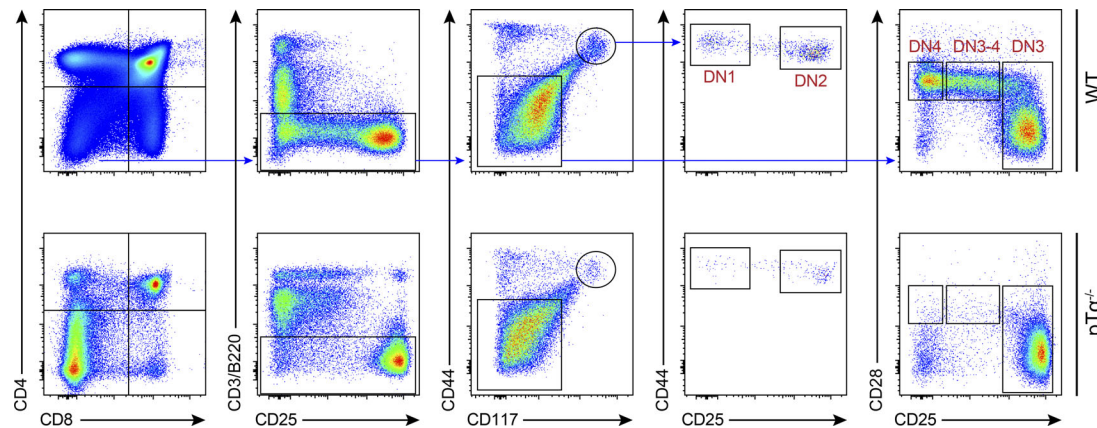
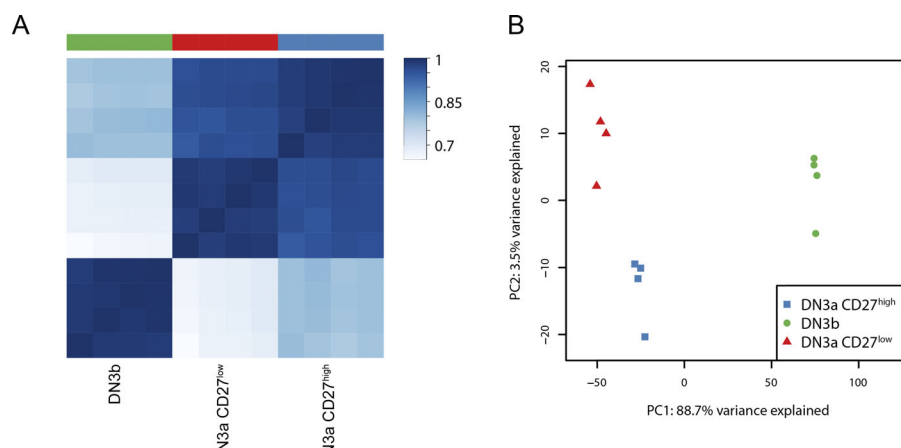


## Supplemental material

Klein et al., <https://doi.org/10.1084/jem.20181444>



**Figure S1. Gating strategy for identification of DN stages.** Representative FACS plots showing the gating strategy to identify DN stages in WT (top) and pTa<sup>-/-</sup> (bottom) mice. The different populations were all defined as CD4<sup>-</sup>CD8<sup>-</sup>CD3<sup>-</sup>B220<sup>-</sup> and additionally as follows: DN1: CD25<sup>high</sup>CD44<sup>high</sup>CD117<sup>high</sup>; DN2: CD25<sup>high</sup>CD44<sup>high</sup>CD117<sup>high</sup>; DN3: CD25<sup>high</sup>CD44<sup>low</sup>CD117<sup>low</sup>; DN3-4: CD25<sup>int</sup>CD44<sup>low</sup>CD117<sup>low</sup>CD28<sup>+</sup>; and DN4: CD25<sup>low</sup>CD44<sup>low</sup>CD117<sup>low</sup>CD28<sup>+</sup>. Two independent experiments were performed, with representative data from one experiment shown.



**Figure S2. Gene expression analysis of WT DN3a CD27<sup>high</sup>, DN3a CD27<sup>low</sup>, and DN3b cells.** Bulk RNA-seq on DN3a CD27<sup>high</sup>, DN3a CD27<sup>low</sup>, and DN3b cells, performed as described in Materials and methods. **(A)** Heat map of Spearman correlation coefficients across samples (using the 25% most variable genes). **(B)** Projection of the samples on the two first axes of a PCA (based on 25% most variable genes).

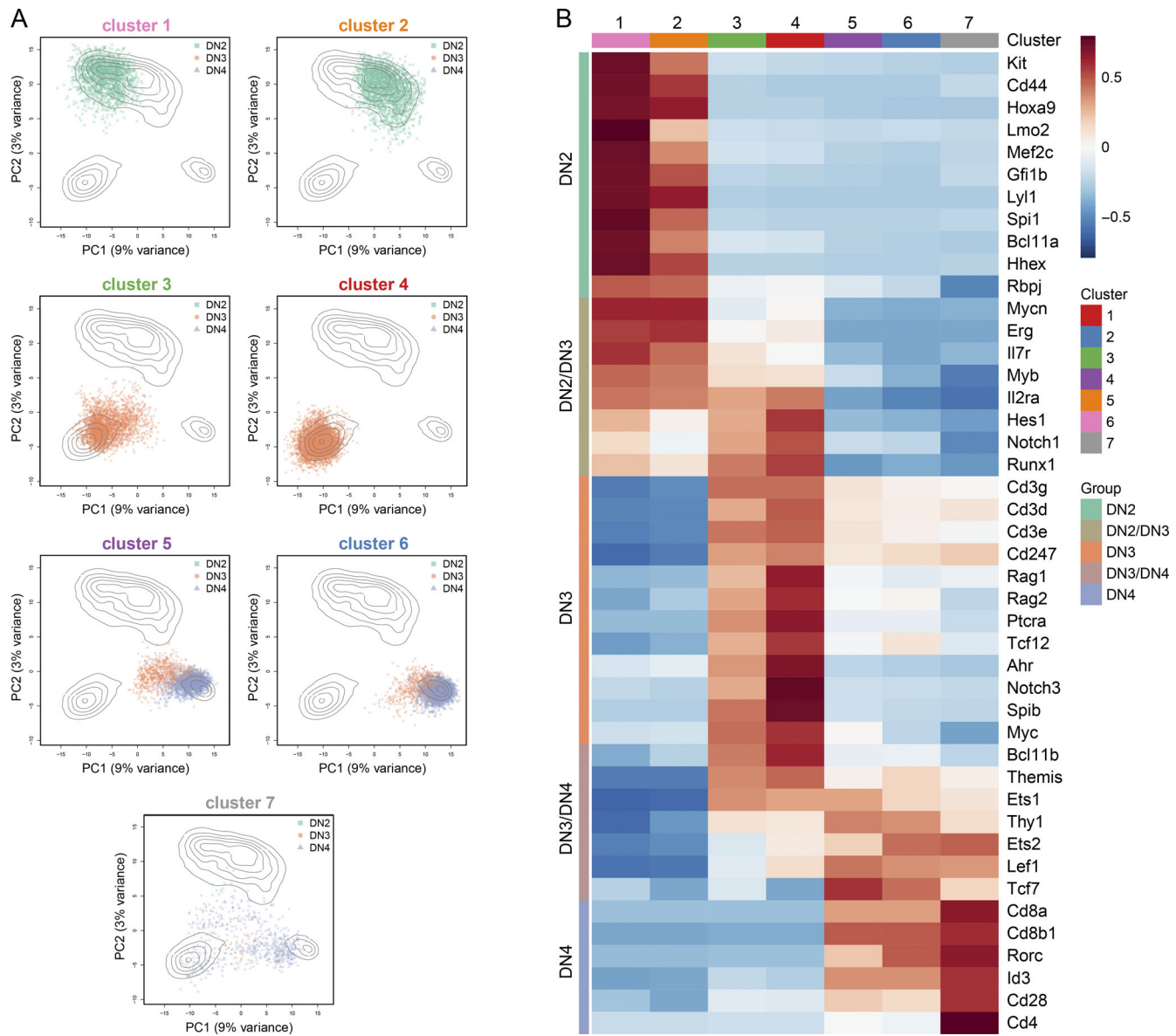


**Figure S3. Single-cell RNA-seq-based clustering of DN2, DN3, and DN4 cells.** Single-cell RNA-seq of DN2, DN3, and DN4 cells, performed as described in Materials and methods. **(A)** Projection of the cells belonging to each cluster on the two first components of a PCA. Colors represent the different populations. Contour lines represent the density of the DN2, DN3, and DN4 cells in the PCA space. **(B)** Heat map of average expression across cells of each cluster of marker genes involved in T cell development, grouped based on their known expression profile in DN2, DN2/DN3, DN3, DN3/DN4, or DN4 cells, for the different clusters. The color gradient indicates the centered and scaled average normalized log-counts of each marker across all cells from each cluster.

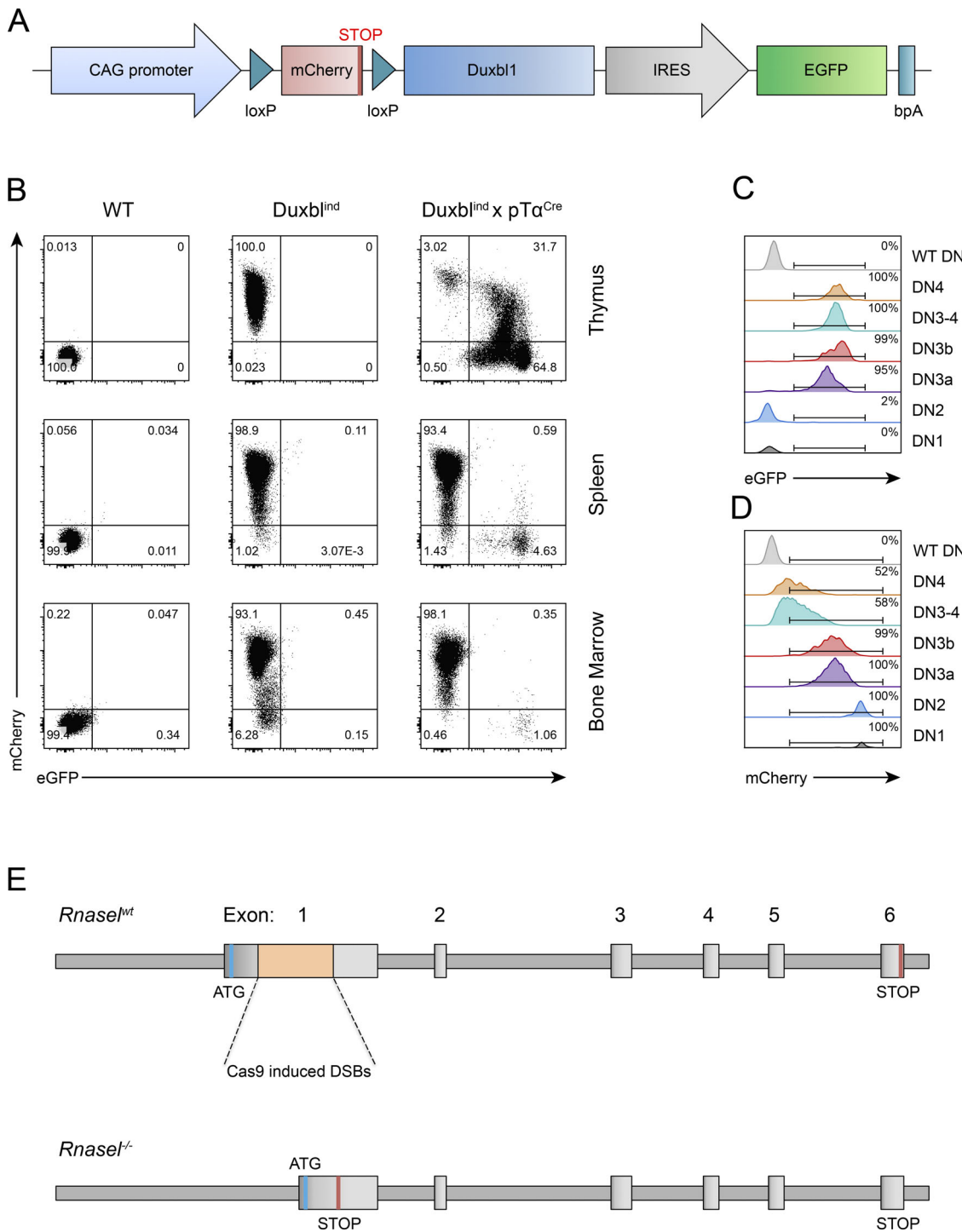


**Figure S4. Generation of conditional Duxbl transgenic and Rnasel<sup>-/-</sup> mice.** **(A)** Schematic figure of the construct used for the generation of conditional Duxbl transgenic mice. CAG promoter driving the expression is followed by an mCherry stop-cassette that is flanked by lox-P sites, followed by Duxbl1 cDNA coupled via an internal-ribosomal-entry-site (IRES) to the eGFP gene, ending with the bovine growth hormone polyadenylation site (bpA). **(B)** Representative FACS plots of mCherry and eGFP expression in the thymus (top), spleen (middle), and bone marrow (bottom) of WT, Duxbl<sup>Ind</sup>, and Duxbl<sup>Ind</sup>xpTa<sup>Cre</sup> mice. **(C and D)** Representative histograms showing the frequencies of eGFP-positive (C) and mCherry-positive (D) cells of DN1, DN2, DN3a, DN3b, DN3-4, and DN4 cells in the thymus of Duxbl<sup>Ind</sup>xpTa<sup>Cre</sup> mice, and WT DN cells. **(E)** Schematic figure of the genome editing performed for the generation of Rnasel<sup>-/-</sup> mice. Two double-strand breaks (DSBs) were introduced in exon 1 of the Rnasel gene using the CRISPR/Cas9 system. This resulted in a 328-bp deletion, thereby inducing a frame shift and a premature stop-codon (STOP). For analysis, mice were bred to homozygosity. Gate numbers in FACS plots and histograms indicate frequencies of parent gate. DN stages were identified by FACS as shown in Fig. S1.

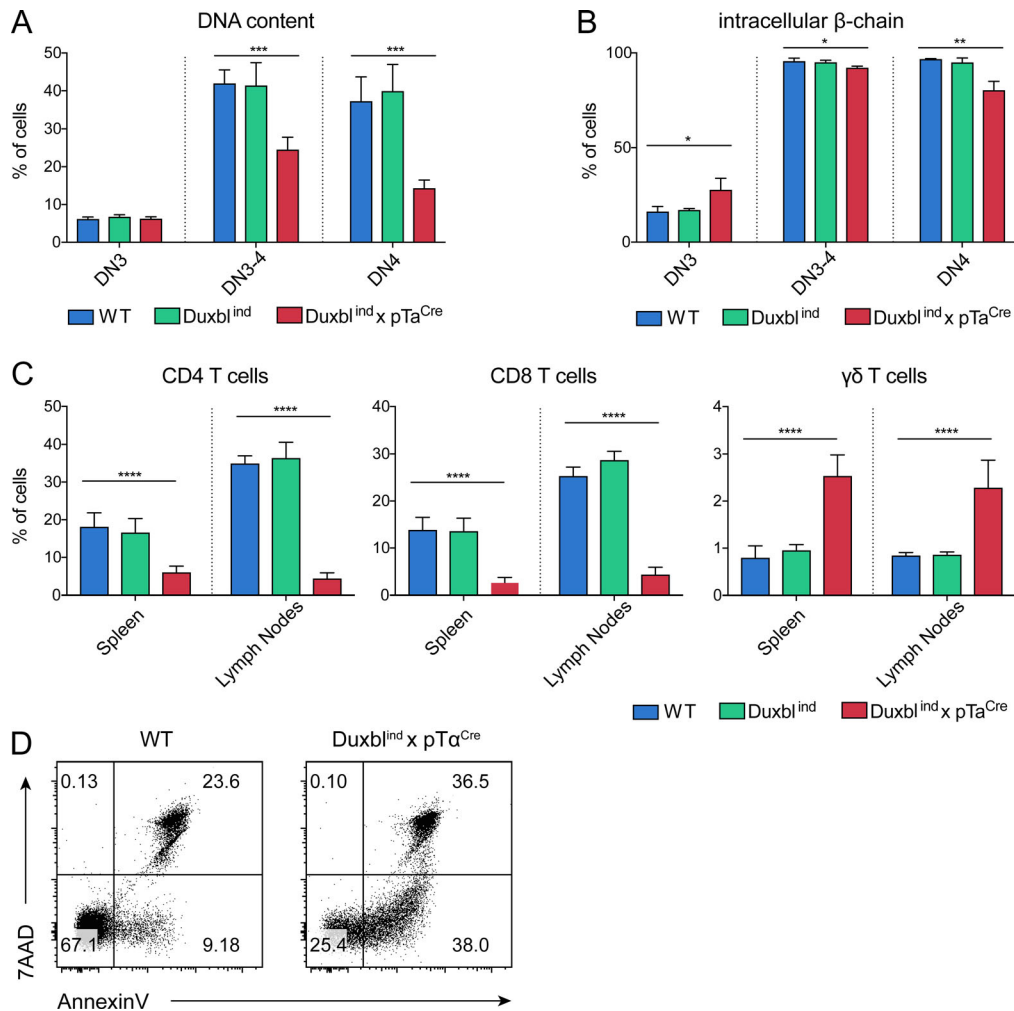


**Figure S5. Analysis of Duxbl<sup>ind</sup>xpTa<sup>Cre</sup> mice.** **(A)** Frequency of cells in cycle in DN3, DN3–4, and DN4 cells of WT and Duxbl<sup>ind</sup>xpTa<sup>Cre</sup> mice based on the content of DNA in each cell detected by FACS. **(B)** Frequency of cells positive for intracellular  $\beta$ -chain expression in DN3, DN3–4, and DN4 cells of WT and Duxbl<sup>ind</sup>xpTa<sup>Cre</sup> mice. **(C)** Frequencies of CD4 T cells (left), CD8 T cells (middle), and  $\gamma\delta$ -T cells (right) in the spleen and lymph nodes of WT (spleen:  $n = 6$ , lymph nodes:  $n = 4$ ), Duxbl<sup>ind</sup> (spleen:  $n = 5$ , lymph nodes:  $n = 4$ ), and Duxbl<sup>ind</sup>xpTa<sup>Cre</sup> (spleen:  $n = 6$ , lymph nodes:  $n = 4$ ) mice. **(A–C)** Data were collected from four (A and B) or three (C) independent experiments. **(D)** Representative FACS plots of sorted DN3 cells from WT and Duxbl<sup>ind</sup>xpTa<sup>Cre</sup> mice after 3 d of culture showing living, early apoptotic, and late apoptotic cells based on annexinV and 7AAD expression of sorted DN3 cells from WT and Duxbl<sup>ind</sup>xpTa<sup>Cre</sup> mice. Living cells were defined as annexinV<sup>-</sup> 7AAD<sup>-</sup>, early apoptotic cells as annexinV<sup>+</sup> 7AAD<sup>-</sup>, and late apoptotic cells as annexinV<sup>+</sup> 7AAD<sup>+</sup>. Three independent experiments were performed, with representative data from one experiment shown. Gate numbers in FACS plots indicate frequencies of parent gate. DN stages were identified by FACS as shown in Fig. S1. Statistical analysis was done with two-tailed unpaired Student's *t* test. \*,  $P < 0.05$ ; \*\*,  $P < 0.01$ ; \*\*\*,  $P < 0.001$ ; \*\*\*\*,  $P < 0.0001$ . Error bars indicate standard deviation.